



Synthesis of carbon nanowalls on the surface of nanoporous alumina membranes by RI-PECVD method

Yerassyl Yerlanuly^{a,*}, Dennis Christy^b, Ngo Van Nong^b, Hiroki Kondo^b, Balaussa Alpysbayeva^a, Renata Nemkayeva^c, Meruert Kadyr^a, Tlekkabul Ramazanov^c, Maratbek Gabdullin^{c,d}, Didar Batryshev^{a,e}, Masaru Hori^b

^a Laboratory of Engineering Profile at Al-Farabi Kazakh National University, al-Farabi ave.71, Almaty 050040, Kazakhstan

^b Center for Low-temperature Plasma Sciences, Nagoya University, Furo-cho, Chikusa-ku, Nagoya 464-8603, Japan

^c National Nanotechnology Laboratory Open Type at Al-Farabi Kazakh National University, al-Farabi ave.71, Almaty 050040, Kazakhstan

^d Kazakh-British Technical University, Tole bi st. 59, Almaty 050000, Kazakhstan

^e Kh. Dosmukhamedov Atyrau State University, Studenchesky ave. 212/1, Atyrau 060011, Kazakhstan

ARTICLE INFO

Keywords:

Carbon nanowalls
Radical-injection plasma enhanced chemical vapor deposition
Nanoporous alumina membrane
Raman spectrum
Scanning electron microscopy

ABSTRACT

This work is devoted to the synthesis of carbon nanowalls on the surface of a nanoporous aluminum oxide membrane by radical-injection plasma enhanced chemical vapor deposition method. Nanoporous alumina oxide membranes with different morphology and thickness, which were obtained by the method of two-stage electrochemical anodization, were used as a substrate. For comparative analysis, carbon nanowalls were also obtained on the surface of a silicon substrate and aluminum foil. The synthesized nanostructures were investigated by using scanning electron microscopy and Raman spectroscopy. The dependence of the morphology and height of carbon nanowalls on the pore size and the thickness of the alumina membrane, respectively, was revealed.

1. Introduction

Nowadays, various allotropic modifications of carbon nanomaterials are of great interest in scientific community due to their unique physical and chemical properties [1–8]. One of the promising carbon nanostructures is carbon nanowalls (CNWs) which owing to the structural, electrical, optical, and mechanical properties [3,8–9] has a wide area of application as supercapacitors [10], sensors and electronics [11–12], etc. CNWs are known as vertical graphene nanosheets [13–16], which have three-dimensional structure and represent a form of labyrinth (maze-like) surface with vertically oriented graphene nanosheets that are freely perpendicular to the substrate. One of the features of the CNWs is that for their synthesis the catalysts are not required, unlike for carbon nanotubes. Hence, they can be synthesized on the substrates of various materials [17–21], such as metals (stainless steel, Pt, Ti, Cu, Ni, Mo, Zr, Hf, Nb, W) semiconductors (Si) and even on insulators (Al₂O₃, quartz). Due to the large surface area, CNWs are potential candidate material for using as electrodes in lithium-ion batteries, as electron field emitters, as catalyst supports in fuel cells, and as an electrode or active material in solar cell [22]. In this relation, morphology of CNWs plays one of the important roles in such applications. Indeed, V.A. Krivchenko

et al. in [9] reported that CNWs with structural imperfections, presence of edge states and high surface density can demonstrate remarkable optical properties; thereby the total reflectance can reach up to 0.13%, which exceeds that of carbon nanotube forest. Further, H.J. Cho et al. showed that the electrical conductivity of CNWs depends on their linear density (number of walls per micron), wherein an increase in density leads to an improvement in electrical properties [23]. Thus, control of the growth of CNWs is a very urgent task and there is a lot of reports on this topic [23–26] related to the study of the influence of plasma parameters on their growth. And all of them are aimed at obtaining nanowalls with certain structural and geometric characteristics. In this paper, we propose another method for controlling the growth of CNWs, i.e. control of nanowall growth along a known trajectory (in a certain order) by using nanoporous membranes.

The nanoporous membrane is another type of perspective nanomaterials, with one of the distinct representatives – nanoporous aluminum oxide (alumina), that is widely used for drug delivery, catalysis, energy storage, sensors and various biological applications [27–28]. Besides, nanoporous aluminum oxide membranes are used as templates for the fabrication of various nanostructures, such as nanofibers, nanotubes, nanoparticles etc. with the very specific and controlled

* Corresponding author.

E-mail address: yerlanuly@physics.kz (Y. Yerlanuly).

<https://doi.org/10.1016/j.apsusc.2020.146533>

Received 15 October 2019; Received in revised form 23 February 2020; Accepted 28 April 2020

Available online 30 April 2020

0169-4332/ © 2020 Elsevier B.V. All rights reserved.

geometry [28–30].

In this work, synthesis of carbon nanowalls on the surface of the nanoporous aluminum oxide membrane by radical-injection plasma enhanced chemical vapor deposition (RI-PECVD) method is considered. Since both carbon nanowalls and nanoporous membranes are very interesting for the future applications, the complex study of their combined properties, particularly growth mechanisms, will give us a new direction of research. For these purposes, the effect of the pore size and thickness of the aluminum oxide membrane on the growth of the CNWs was considered.

2. Experimental part

2.1. Obtaining nanoporous alumina membranes

To obtain a nanoporous alumina membrane, a two-stage method of electrochemical anodization was used [31]. Initial aluminum foil (99.99% purity) with thickness of 50 μm was previously cleaned by acetone, boiled in ethanol and dried in oven at 105 $^{\circ}\text{C}$. After that the foil was annealed in the muffle furnace at $t = 500$ $^{\circ}\text{C}$ for 3 h in air. Anodizing process was carried out in a specially made fluoroplastic cell at the bottom of which aluminum foil was attached to the large metal holder (anode) for its effective cooling.

The cell was filled by electrolyte – 0.4 M aqua solution of oxalic acid H_3PO_4 into which a tungsten electrode (the cathode) was plunged. The electrolyte solution during the anodization process is stirred with a magnetic stirrer. The morphology (pore size) and the thickness of the resulting nanoporous membranes can be controlled by changing the temperature and electrical voltage of the anodization. As a result of the experiment, membranes with various pore sizes and thickness are formed (as seen in the SEM images in Fig. 2).

2.2. Synthesis of CNWs by RI-PECVD method

As is mentioned above, the synthesis of CNWs on the surface of nanoporous alumina membrane was carried out by RI-PECVD method. The experimental setup and operation steps are well described in [32–34]. RI-PECVD method uses two plasma sources. The first one is the upper one, microwave plasma (MWP) generated with frequency of 2.45 GHz by microwave oven and power of 400 W, supplied through a quartz window. The second one is the lower one, capacitively coupled plasma (CCP) with parallel electrode system generated with frequency of 100 MHz (very high frequency; VHF) and power of 1–400 W. The generation of hydrocarbon radicals occurs in the following steps: hydrogen gas (H_2) is introduced into the MWP region for formation of H atoms, which then flew into the lower CCP region through the “showerhead” type electrode system, then methane gas (CH_4) is introduced into the working chamber through the showerhead electrode to generate hydrocarbon radicals. The ratio of the flow rates of CH_4 to H_2 in this study was maintained at 1:2, i.e. 50 and 100 sccm, respectively. The CH_4/H_2 ratio is important parameter for controlling the structure of carbon materials. During the process, the pressure in the evacuation position was maintained at 1 Pa to suppress the loss of ion bombardment energy during ion collisions. The surface temperature of the substrate was 500 $^{\circ}\text{C}$, the synthesis time was 10 min. Nanoporous aluminum oxide of various pore size and thickness was used as a substrate. Also, aluminum foil and silicon substrate were used for comparison of CNWs syntheses.

3. Results and discussion

The obtained samples of CNWs were investigated by using scanning electron microscopy (SEM) and Raman spectroscopy. Fig. 2 shows the results of SEM analysis of CNWs synthesized on the surface of aluminum foil and silicon substrate. The CNWs on the surface of a silicon substrate have a denser appearance compared with the ones

synthesized on aluminum foil. Moreover, it can be noticed, that CNWs on Si demonstrate a petal-like structure, while CNWs on Al have a maze-like configuration.

Fig. 3 shows the results of SEM analysis of the CNWs synthesized on the surface of nanoporous alumina with different pore sizes and thicknesses. As can be seen from Fig. 3a, b and c, the morphologies of the CNWs on the surface of alumina membrane with pore sizes of 114, 155 and 169 nm are same and practically unchanged from that of the CNWs obtained on aluminum foil. Interesting results were obtained in case of using substrates with pore sizes of 200 and 75 nm. One can see that in case of pore size of 200 nm the density of the CNWs looks higher due to the shorter length of walls and also the gaps between nanowalls (similar size of initial pores of alumina membrane) can be observed (Fig. 3d). It seems that this image well confirms the early conventional theory of the growth mechanism of nanowalls that at the beginning of growth process, randomly oriented carbon flakes start to grow mainly in the horizontal direction and then few vertical CNWs grow continuously forming a bigger one. However, the morphology of the membrane differs from the morphology of the silicon substrate. In this case, the difference in the growth mechanism of nanowalls appears. We believe that the pore size and the surface of the membrane have a very strong effect on the initial growth of nanowalls. If to compare the membranes shown in Fig. 1, it's seen that the smaller the pore size of the membranes, the larger the surface for the formation of the interface layer and the growth of nanowalls. Does it mean that the density of the nanowalls will be less if the surface area of the membrane for the formation of nanowalls nuclei is smaller? In fact, it turned out the opposite (Fig. 3d and e). In the case of a smaller pore size of the membrane (75 nm), the nanowalls growth mechanism is similar to that described above. At the same time, at the beginning of growth, carbon flakes can grow both in vertical and horizontal directions due to the surface curvature of the membrane at the edge of the pores. Indeed, Fig. 3e2 shows that the pores of the membranes are closed by nanowalls and their roots are combined. In the case of a membrane with large pores, the vertical growth mechanism of carbon flakes strongly prevails compared to the horizontal one. In this case, the growth of each flake is carried out independently, forming individual nanowalls and thus increasing their density (Fig. 3d). SEM images of cross section of all samples are shown in Fig. 3a1–3e1. The values of average length, height and pore surface density of CNWs synthesized on alumina membranes with different diameter of pores and thicknesses are shown in Table 1. It's seen that for samples #2–4 with closer characteristics (pore diameters and thicknesses of membranes) the average lengths and pore surface densities of synthesized CNWs are more similar, than for samples #1 and #5, which have significant differences by parameters from those samples. At the same time, there is a quite clear tendency to increase and decrease the pore surface density and the average length of CNWs with an increase and decrease in pore diameter of alumina membranes, respectively. Obtained results are in good correlation with our explanation of the growth mechanism of CNWs on the surface of the membrane. It is seen that the values of thickness of the nanoporous aluminum oxide substrate are in range of 3–18 μm , whereas the heights of the CNWs are in range of 85–907 nm. It was found that the increase in alumina thickness leads to a decrease in height of the CNWs. This phenomenon can be explained by the fact that thermal and electrical conductivity of the nanoporous substrate changes depending on its thickness and due to this, the height of the synthesized CNWs changes too. A similar result was obtained by authors in work [17], they studied how a type of substrate can affect the synthesis of CNWs and found that for the same synthesis time the growth speed of CNWs on insulators is much lower compared with that on metals (see Fig. 4).

The Raman spectra of the obtained samples are shown in Fig. 5, which fully correspond to the typical spectrum of CNWs with pronounced D, G, D', G' (2D), G + D peaks. The D mode is associated with defects in sp^2 structures, the G mode is usually observed in graphite materials, the D' peak corresponds to the violation of the symmetry of

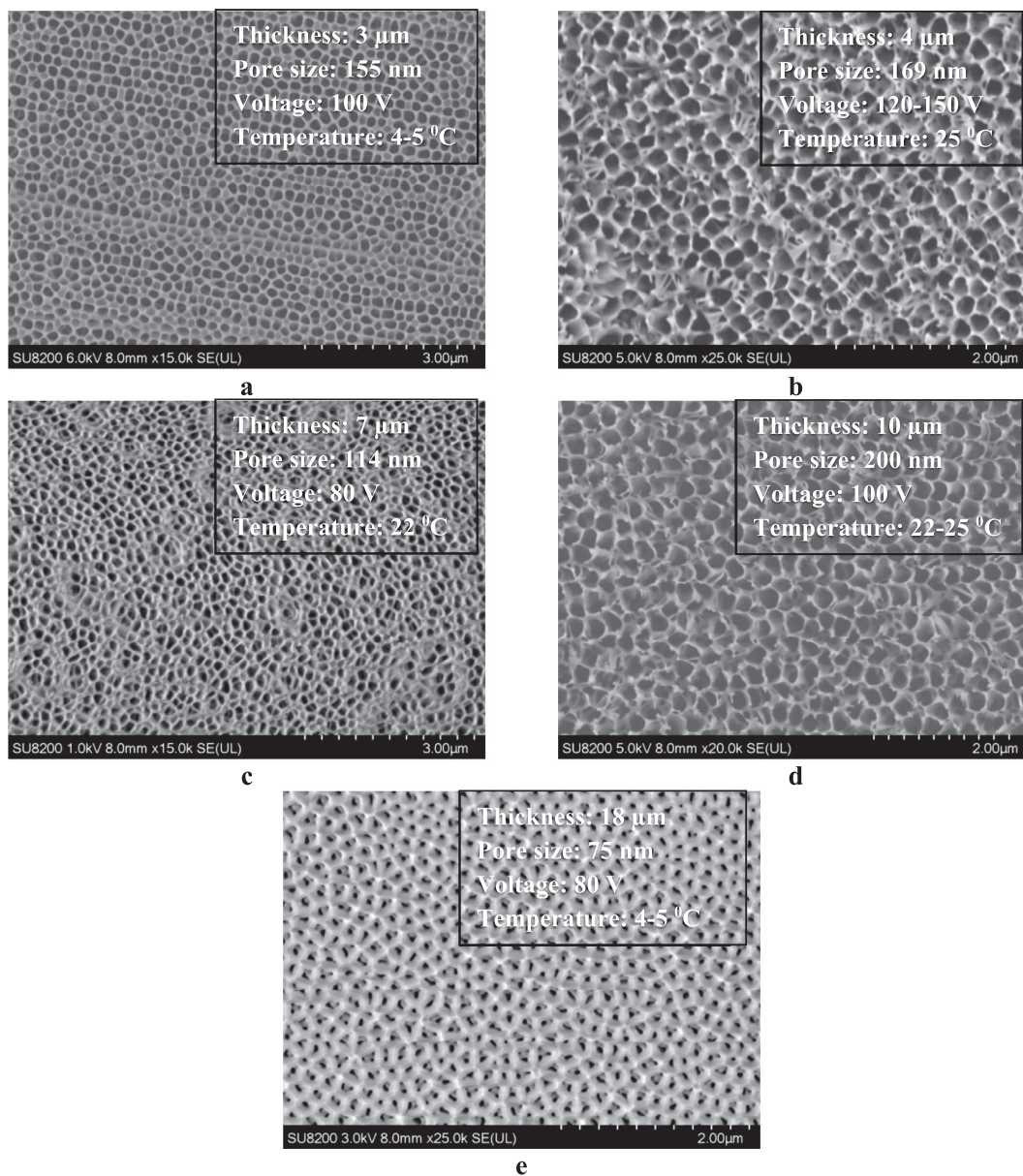


Fig. 1. SEM image of the alumina membranes obtained at different temperature and voltage values.

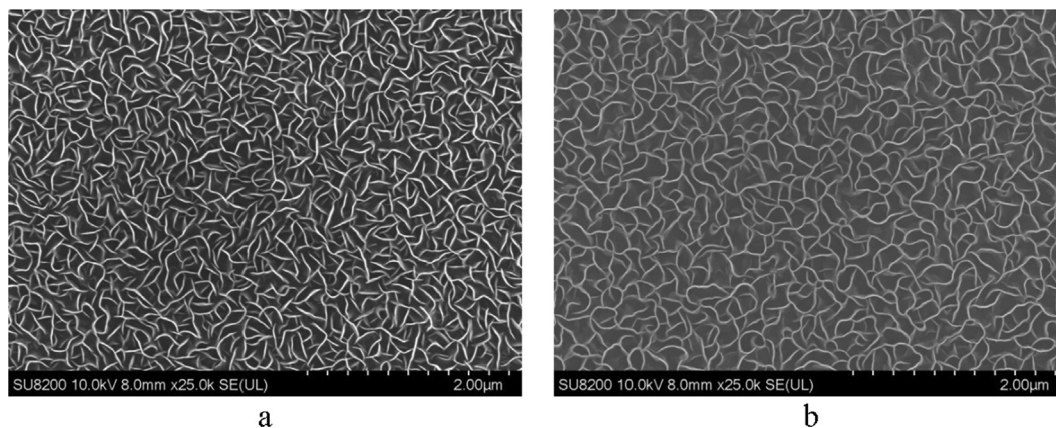


Fig. 2. SEM image of the CNWs on the surface of a silicon substrate (a) and aluminum foil (b).

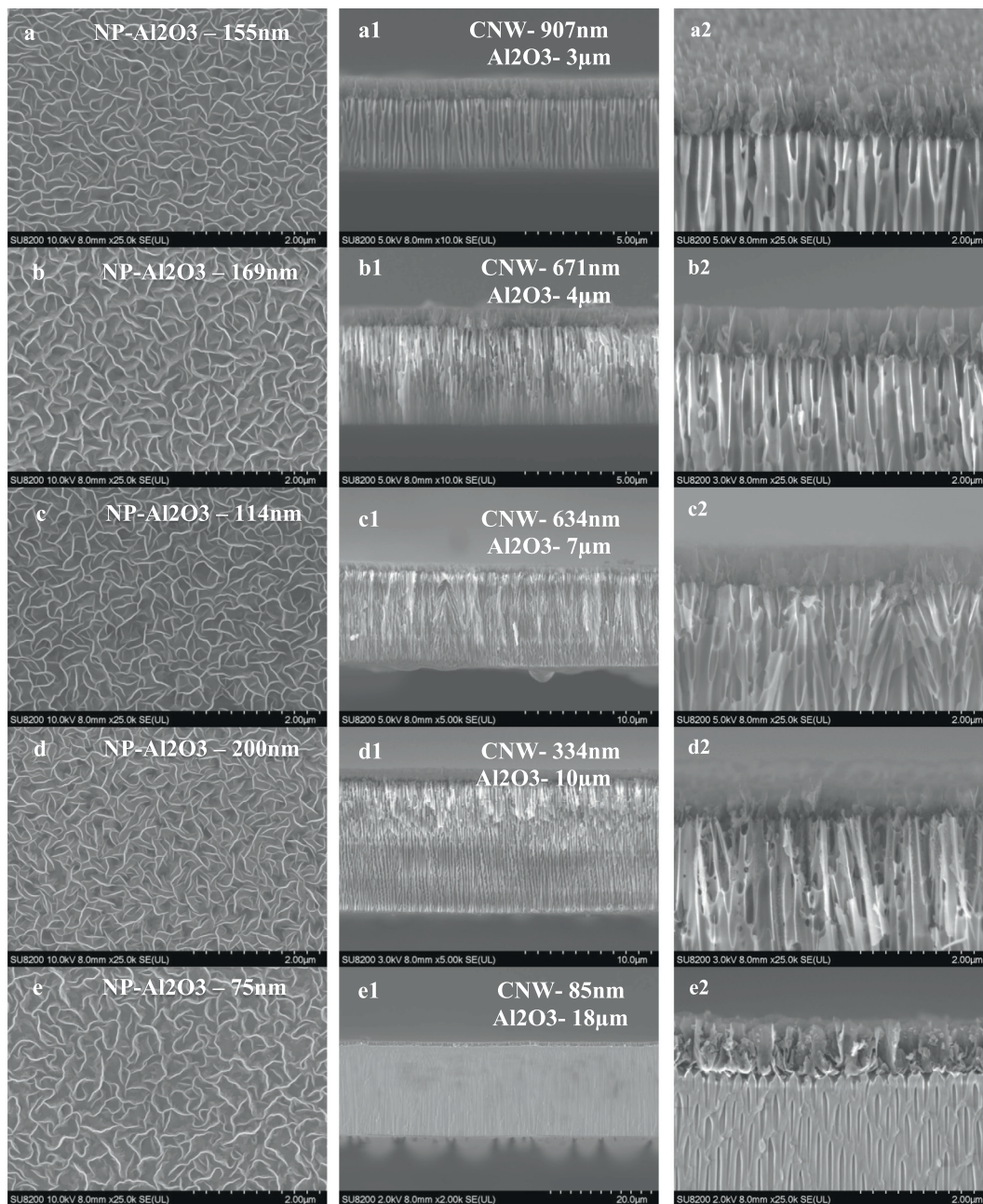


Fig. 3. SEM image of the CNWs on the surface of nanoporous alumina membranes with different pore sizes and thicknesses (the pore sizes as well as the thickness of membranes and the height of CNWs are given in the left and middle columns, respectively).

the final size of the sp^2 crystal and the appearance of graphene edges, the G' peak (2D) is the second-order of the D mode (appearance of 2D-peak, considered as a fingerprint of carbon material, crystalline) and peak G + D (D'') is a band of a combination of G and D peaks. Table 2 presents the ratio of the intensities of the peaks D and G (I_D/I_G), D' and

G ($I_{D'}/I_G$), 2D and G (I_{2D}/I_G). As can be seen, the ratio of D and G peaks (I_D/I_G), which indicates the degree of imperfection in the structure [35], is practically the same in all samples, except for the sample where the thickness of nanoporous aluminum is 10 μm and the height of the CNWs is 334 nm, in this case, a significant defective structure is

Table 1
The main characteristics of CNWs synthesized on alumina membranes with different pore sizes and thicknesses.

Samples	Diameter of pores of alumina membranes, nm	Thickness of alumina membranes, μm	Average length of CNWs, nm	CNWs pore surface density, $1/\mu\text{m}^2$	Height of CNWs, nm
#1	75	18	443	17	85
#2	114	7	351	26	634
#3	155	3	346	28	907
#4	169	4	371	23	671
#5	200	10	314	32	334

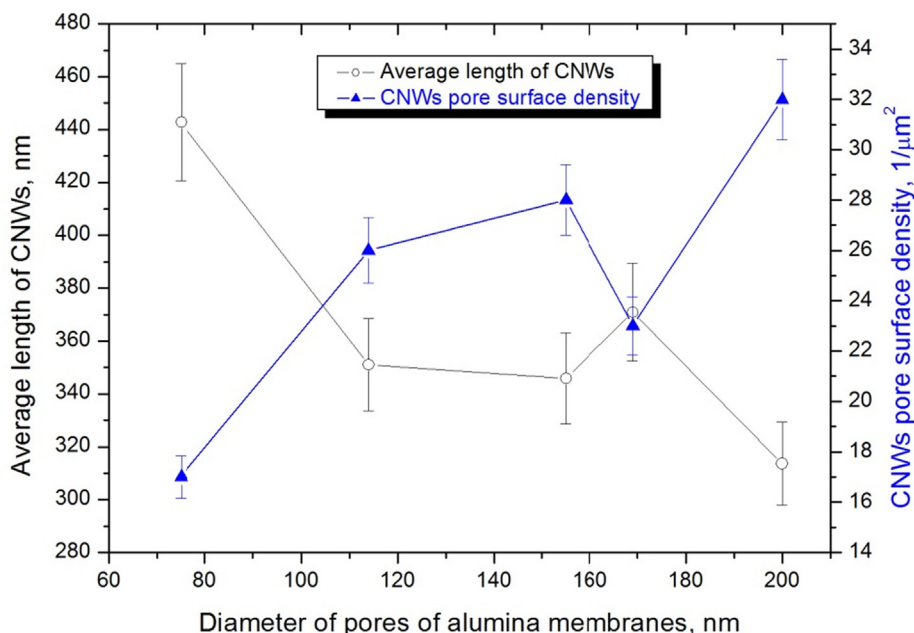


Fig. 4. The dependence of the average length and pore density of CNWs.

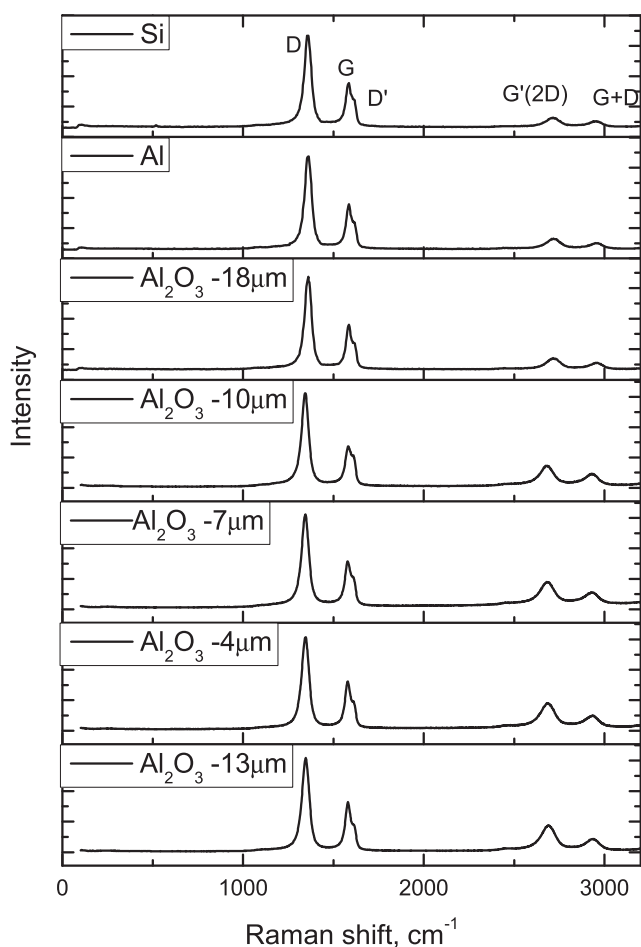


Fig. 5. Raman spectra of CNWs synthesized on alumina substrates with different thicknesses.

observed. Apparently, the highest values of $I_{D'}/I_G$ (2.28) and $I_{D'}/I_G$ can be explained by the largest diameter of alumina pores (200 nm) that define the defective structure of initial small graphite grains. It is also

interesting to notice, that CNWs grown on Al foil, Si substrate and Al_2O_3 with the smallest (75 nm) pores have the lower I_{2D}/I_G values comparing with that of CNWs grown on the rest Al_2O_3 porous membranes. This can indicate that the walls forming on highly porous alumina substrates are thinner, i.e. have the lower number of graphene layers, due to the higher speed of the vertical growth.

4. Conclusion

In this work, the synthesis of CNWs on the surface of nanoporous alumina membrane by RI-PECVD method was considered. The influence of the pore sizes and thicknesses of the nanoporous aluminum oxide substrate on the height, morphology, and structural characteristics of the synthesized CNWs was studied. It was found that the increase in alumina thickness leads to the decrease in height of the CNWs. Estimated ratio of D and G peaks (I_D/I_G), which indicates the degree of imperfection in the structure, showed the same values in all samples, except for the sample where the thickness of nanoporous aluminum is 10 μm and the height of the CNWs is 334 nm, in this case, a significant defective structure is observed. Interesting result was obtained in case of CNWs synthesis on the surface of aluminum oxide membrane with pore size of 200 nm. It was found that the wider pore size the more visible the initial pore of alumina, i.e. the more perfectly CNWs replicate (or reproduce) the surface structure of nanoporous membrane. It was determined that the walls forming on highly porous alumina substrates are thinner, i.e. have the lower number of graphene layers, due to the higher speed of the vertical growth.

CRediT authorship contribution statement

Yerassyl Yerlanuly: Experimental part, Formal analysis, Writing - review & editing, Methodology, Conceptualization. **Dennis Christy:** Experimental part the synthesis of carbon nanowalls. **Ngo Van Nong:** Experimental part the synthesis of carbon nanowalls. **Hiroki Kondo:** Experimental part the synthesis of carbon nanowalls. **Balaussa Alpybayeva:** Experimental part the obtaining nanoporous alumina. **Renata Nemkayeva:** Raman analysis of carbon nanowalls. **Meruert Kadyr:** Experimental part the obtaining nanoporous alumina. **Tlekkabul Ramazanov:** Project administration in Kazakhstan. **Maratbek Gabdullin:** Funding acquisition. **Didar Batryshev:**

Table 2
Raman spectrum characteristics of synthesized CNWs.

Samples and thicknesses of Al ₂ O ₃	Diameter of pores of Al ₂ O ₃ , nm	CNWs heights, nm	Peak positions					I _D /I _G	I _{D'} /I _G	I _{2D} /I _G
			D	G	D'	2D	G + D			
Al ₂ O ₃ -3 μm	155	907	1346	1580	1612	2690	2940	1.89	0.54	0.53
Al ₂ O ₃ -4 μm	169	671	1346	1578	1613	2860	2927	1.90	0.58	0.56
Al ₂ O ₃ -7 μm	114	634	1344	1578	1611	2679	2927	1.98	0.66	0.57
Al ₂ O ₃ -10 μm	200	334	1343	1583	1610	2680	2931	2.28	0.78	0.53
Al ₂ O ₃ -18 μm	75	85	1361	1586	1611	2715	2962	1.88	0.68	0.40
Aluminum foil			1360	1586	1617	2718	2963	1.88	0.66	0.37
Silicon substrate			1361	1586	1611	2718	2965	1.88	0.69	0.36

Supervision in Kazakhstan. **Masaru Hori:** Supervision in Japan.

Declaration of Competing Interest

The authors declare that they have no known competing financial interests or personal relationships that could have appeared to influence the work reported in this paper.

References

- [1] P. Hojati-Talemi, G.P. Simon, Carbon 49 (8) (2011) 2869–2877.
- [2] J.H. Chen, W.Z. Li, D.Z. Wang, S.X. Yang, J.G. Wen, Z.F. Ran, Carbon 40 (8) (2002) 1193–1197.
- [3] K. Bo, G. Yu, P. Lu, S. Wang, Mao, J. Chen, Carbon 49 (6) (2011) 1849–1858.
- [4] S.A. Orazbayev, M. Henault, T.S. Ramazanov, L. Boufendi, D.G. Batryshev, M.T. Gabdullin, IEEE Trans. Plasma Sci. 47 (7) (2019) 3069–3073.
- [5] S. Orazbayev, M. Gabdullin, T. Ramazanov, M. Dosbolayev, D. Omirbekov, Y. Yerlanuly, Appl. Surf. Sci. 472 (1) (2019) 127–134.
- [6] S.A. Orazbayev, A.U. Utegenov, A.T. Zhunisbekov, M. Slamyiya, M.K. Dosbolayev, T.S. Ramazanov, Contrib. Plasma Phys. 58 (10) (2018) 961–966.
- [7] Y.A. Ussenov, A.S. Pazył, M.K. Dosbolayev, M.T. Gabdullin, T.T. Daniyarov, M.M. Muratov, T.S. Ramazanov, IEEE Trans. Plasma Sci. 47 (8) (2019) 4159–4164.
- [8] Y. Wu, P. Qiao, T. Chong, Z. Shen, Adv. Mater. 14 (2002) 64–67.
- [9] V.A. Krivchenko, S.A. Evlashin, K.V. Mironovich, N.I. Verbitskiy, A. Nefedov, C. Woll, A.Ya. Kozmenkova, N.V. Suetin, S.E. Svyakhovskiy, D.V. Vyalik, A.T. Rakhimov, A.V. Egorov, L.V. Yashina, Sci. Rep. 3 (2013) 3328.
- [10] S.Y. Kim, et al., J. Trans. Electr. Electron. Mater. 16 (2015) 198–200.
- [11] Paola Russo, Ming Xiao, Norman Y. Zhou, Carbon 120 (2017) 54–62.
- [12] M. Tomatsu, M. Hiramatsu, J.S. Foord, H. Kondo, K. Ishikawa, M. Sekine, K. Takeda, M. Hori, Jpn. J. Appl. Phys. 56 (2017) p. 06HF03.
- [13] S. Ghosh, G. Sahoo, S.R. Polaki, N.G. Krishna, M. Kamruddin, T. Mathews, J. Appl. Phys. 122 (2017) 214902.
- [14] J. Zhao, M. Shaygan, J. Eckert, M. Meyyappan, M.H. Rummeli, Nano Lett. 14 (2014) 3064–3071.
- [15] M. Hiramatsu, M. Hori, Carbon Nanowalls: Synthesis and Emerging Applications, Springer, 2010, 161 pages.
- [16] M. Hiramatsu, K. Shiji, H. Amano, M. Hori, Appl. Phys. Lett. 84 (23) (2004) 4708–4710.
- [17] S. Ghosh, K. Ganesan, S.R. Polaki, Tom Mathews, Sandip Dhara, M. Kamruddin, A.K. Tyagi, Appl. Surf. Sci. 349 (2015) 576–581.
- [18] R. Vitchev, A. Malesevic, R.H. Petrov, R. Kemps, M. Mertens, A. Vanhulsel, C. Van Haesendonck, Nanotechnology 21 (2010) 095602.
- [19] D.G. Batryshev, Y. Yerlanuly, T.S. Ramazanov, M.K. Dosbolayev, M.T. Gabdullin, Mater. Today: Proc. 5 (11) (2018) 33764–122769.
- [20] D.G. Batryshev, Y. Yerlanuly, T.S. Ramazanov, M.T. Gabdullin, IEEE Trans. Plasma Sci. 47 (7) (2019) 3044–3046.
- [21] J. Fang, I. Levchenko, T. Laan, S. Kumar, K. Ostrikov, Carbon 78 (2014) 627–632.
- [22] Zishan Husain Khan, Nanomaterials and their applications, Springer Nature Singapore Pte Ltd, 2018, 429 pages.
- [23] H.J. Cho, H. Kondo, K. Ishikawa, M. Sekine, M. Hiramatsu, M. Hori, Carbon 68 (2014) 380–388.
- [24] C.Y. Cheng, K. Teii, IEEE Trans. Plasma Sci. 40 (7) (2012) 1783–1788.
- [25] Sh. Kondo, et al., J. Appl. Phys. 106 (2009) 094302.
- [26] S. Suzuki, A. Chatterjee, Ch.-L. Cheng, M. Yoshimura, Japanese J. Appl. Phys. 50 (2011) 01AF08.
- [27] A. Santos, T. Kumeria, D. Losic, Trends Anal. Chem. 44 (2013) 25–38.
- [28] A.M.M. Jani, D. Losic, N.H. Voelcker, Prog. Mater. Sci. 58 (2013) 636–704.
- [29] S.J. Hurst, E.K. Payne, L. Qin, C.A. Mirkin, Angew. Chem. Int. Ed. Engl. 45 (2006) 2672–2692.
- [30] M.A. Bangar, C.M. Hangarter, B. Yoo, Y. Rhee, W. Chen, A. Mulchandani, N.V. Myung, Electroanal. 21 (2009) 61–67.
- [31] A.P. Ryaguzov, R.R. Nemkayeva, B.E. Alpysbaeva, R.K. Aliaskarov, J. Phys. Conf. Ser. 751 (1) (2016) 012027.
- [32] Shingo Kondo, Masaru Hori, Koji Yamakawa, Shoji Den, Hiroyuki Kano, Mineo Hiramatsu, J. Vacuum Sci. Technol. B Microelectron. Nanometer Struct. 26 (4) (2008) 1294–1300.
- [33] Hirotsugu Sugiura, Lingyun Jia, Hiroki Kondo, Kenji Ishikawa, Takayoshi Tsutsumi, Toshio Hayashi, Keigo Takeda, Makoto Sekine, Masaru Hori, Jpn. J. Appl. Phys. 57 (6S2) (2018) pp. 06JE03.
- [34] Hirotsugu Sugiura, Lingyun Jia, Yasuyuki Ohashi, Hiroki Kondo, Kenji Ishikawa, Takayoshi Tsutsumi, Toshio Hayashi, Keigo Takeda, Makoto Sekine, Masaru Hori, Jpn. J. Appl. Phys. 58 (3) (2019) 030912.
- [35] N. Soin, S.S. Roy, C. O’Kane, J.A.D. McLaughlin, T.H. Limb, C.J.D. Hetherington, Cryst. Eng. Comm. 13 (2011) 312–318.